

Implementation of a Digital Filter Initialization in the WRF Model and Its Application in the Rapid Refresh

STEVEN E. PECKHAM, TATIANA G. SMIRNOVA, STANLEY G. BENJAMIN, JOHN M. BROWN,
AND JAYMES S. KENYON

*NOAA/Earth System Research Laboratory, and Cooperative Institute for Research in Environmental Sciences,
University of Colorado Boulder, Boulder, Colorado*

(Manuscript received 10 June 2015, in final form 2 October 2015)

ABSTRACT

Because of limitations of variational and ensemble data assimilation schemes, resulting analysis fields exhibit some noise from imbalance in subsequent model forecasts. Controlling finescale noise is desirable in the NOAA's Rapid Refresh (RAP) assimilation/forecast system, which uses an hourly data assimilation cycle. Hence, a digital filter initialization (DFI) capability has been introduced into the Weather Research and Forecasting Model and applied operationally in the RAP, for which hourly intermittent assimilation makes DFI essential. A brief overview of the DFI approach, its implementation, and some of its advantages are discussed. Results from a 1-week impact test with and without DFI demonstrate that DFI is effective at reducing high-frequency noise in short-term operational forecasts as well as providing evidence of reduced errors in the 1-h mass and momentum fields. However, DFI is also shown to reduce the strength of parameterized deep moist convection during the first hour of the forecast.

1. Introduction

Atmospheric model initialization refers to the process by which 3D meteorological analyses are modified to minimize initial mass/wind imbalance and subsequent inertia-gravity waves (IGW) in model integrations. By modifying condensation and precipitation processes, IGWs can seriously contaminate the model forecast during the first few hours resulting in numerical instabilities, forecast degradation, unrealistic precipitation, and contamination by spurious features in the short-term forecasts used as the background in subsequent data assimilation cycles degrading the analyses. Digital filter initialization (DFI) is one of the available methods to remove or reduce these initial imbalances (Lynch and Huang 1992).

DFI reduces and/or eliminates high-frequency features, including IGW noise, from the model's initial state by filtering in time. A time series of model states produced through integration either forward or backward is used as input to the digital filter. Providing this

time series as input to a low-pass digital filter produces, at the output time of the digital filter, a numerical state where high-frequency components are significantly reduced. Some challenges are faced when using this initialization methodology. The first challenge lies in selecting the filter's cutoff frequency such that high-frequency noise is removed but meteorologically significant features remain. The optimal cutoff frequency provides a model state in which spurious high-frequency perturbations have been removed and the initial model state is balanced. Another challenge is determining the optimal time filtering interval. A longer time interval results in a sharper filter, but also usurps the computational time otherwise available for the operational forecast.

A backward-forward two-pass DFI application was developed for the NOAA Rapid Update Cycle (RUC) model/assimilation system (Benjamin et al. 2004) where it was found to be essential to reduce accumulating analysis imbalances for an hourly updated intermittent assimilation cycle. Application of the DFI to the RUC model was extended to improve hydrometeor/moisture assimilation in 2006 and subsequently to improve radar reflectivity assimilation (Weygandt and Benjamin 2007; Weygandt et al. 2008).

Corresponding author address: Dr. Steven Peckham, NOAA/ESRL/GSD, 325 Broadway, Boulder, CO 80503.
E-mail: steven.peckham@noaa.gov

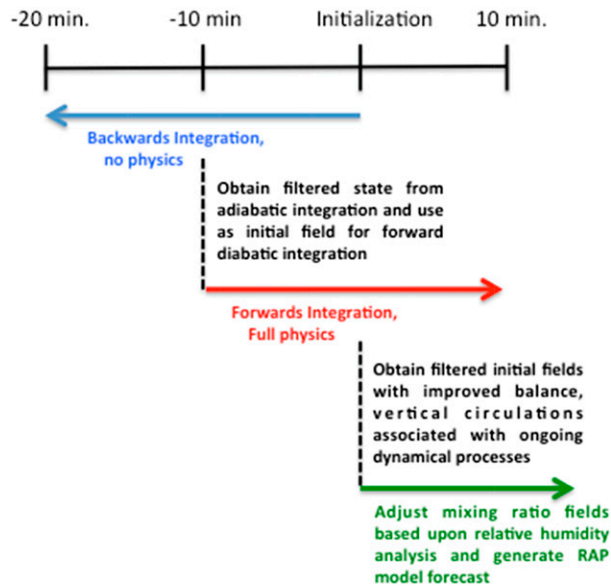


FIG. 1. Schematic diagram illustrating the methodology by which the digital filter initialization (DFI) was implemented within the RAP model. The blue arrow represents the adiabatic backward model integration, the red arrow represents the diabatic forward model integration, and the green arrow represents the forward integration of the RAP using the initial filtered state from the DFI.

In the Weather Research and Forecasting (WRF) Model (Skamarock and Klemp 2008), the DFI is implemented following Huang and Yang (2002) and Weygandt and Benjamin (2007). The WRF DFI implementation supports several different low-pass filter options, including digital filter launching (Lynch and Huang 1994), diabatic DFI (Huang and Lynch 1993), and twice DFI (Lynch 1997; Lynch et al. 1997). The twice DFI (two pass) methodology begins with a backward integration of the model under adiabatic, inviscid conditions from time $t = 0$ to $t = -2T$, where T is 10 min as in Fig. 1 to produce a time series of the model states. These backward integrated fields are filtered (the first DFI pass) to reduce the amplitude of high-frequency modes and produce a model state valid at $t = -T$. The filter is a simple weighted average following Lynch et al. (1997). The filter weights for the Dolph window (Table 1) have the form of a shallow parabola in the interior with the values ranging from approximately 0.011 toward the edge to roughly 0.013 at the center. The filter weights at the edges are much larger; values of approximately 0.318 for the experiments described in this paper.

Next, using this filtered state, the same model with full diabatic and viscid physics enabled is integrated forward producing a second time series from $t = -T$ to $t = T$. This second time series is filtered using the same filter weights to produce the final DFI model state valid at the

TABLE 1. Filter coefficients, or weights, defining the Dolph filter used in the RAP DFI. The positive coefficient numbers are presented with the understanding that they are symmetric about zero.

Coef No.	Filter weight value
0	0.013 060 60
1	0.013 053 20
2	0.013 030 36
3	0.012 992 31
4	0.012 939 42
5	0.012 871 04
6	0.012 788 47
7	0.012 691 12
8	0.012 579 16
9	0.012 453 53
10	0.012 313 45
11	0.012 160 90
12	0.011 994 43
13	0.011 815 80
14	0.011 624 23
15	0.318 162 60

analysis time $T = 0$. Previous studies have shown that DFI results in initial meteorological fields that are more consistently balanced within the context of the forecast model's dynamics, including the elimination of sudden adjustments at the initial time to the cloud water content and vertical velocity, than would otherwise be the case if the analysis were used without modification (Huang and Lynch 1993; Huang and Sundqvist 1993; Chen and Huang 2006).

Several journal articles briefly discuss the use of the WRF DFI (Pan et al. 2014; Zhu et al. 2013, etc.). The goal of this paper is to report on the DFI development in the Rapid Refresh (RAP) model (<http://rapidrefresh.noaa.gov>; Benjamin et al. 2007, 2015, manuscript submitted to *Mon. Wea. Rev.*, hereafter BEN) as well as its state when originally released to the community. The following section describes the development of the DFI in relationship to the operational RAP. Metrics regarding the DFI performance will be used to provide evidence of the overall effectiveness of the DFI in this application. Finally, a discussion on some of the issues with the DFI in operational forecasting, along with a potential solution to the problems, will be presented.

2. DFI development in the RAP and WRF

A two-pass DFI was implemented in the RUC model run at NCEP in 1998 (Benjamin et al. 2004), and used since then, with several modifications, in the operational RUC at NCEP. No special modifications were necessary to apply the DFI to the hydrostatic, hybrid-isentropic vertical coordinate used in the RUC model. Beginning around 2002, NOAA discussions started about the possible transition of the NOAA operational hourly

updated forecast model suite from the RUC to the RAP. This new operational forecast suite would be based upon the WRF community model and the Gridpoint Statistical Interpolation analysis system (GSI). Some RUC techniques, however, including the DFI, were considered requirements to be added to the WRF modeling framework to support the RAP.

An early adaptation of DFI in the WRF Model implemented at NCAR (Huang et al. 2007) required the output of a restart data file at the end of each DFI integration period, as well as separate executions for each phase of the DFI application. This methodology allowed for flexibility in the DFI runtime procedure, as well as several choices in DFI filter window options. Retrospective simulations using GSI data assimilation along with this DFI configuration on a 30-km mesh were conducted for 96 h beginning on 25 January 2000. Results showed reasonable reduction of noise and simulation spinup time, as well as improvement to conventional observation verification scores (e.g., temperature RMS error relative to radiosondes reduced by approximately 0.1 K at 6 h).

Around the same time, the DFI was also being implemented in the Advanced Research version of WRF at the Global Systems Division of the Earth System Research Laboratory (ESRL; Peckham et al. 2008; Smirnova et al. 2009) for use in the RAP. Compared to the NCAR version of DFI, the ESRL version of DFI was better suited for use in real time or operational forecasting since the filtered states remained in computer memory during the two integration periods, thus requiring no additional output data and significantly decreasing the computational runtime of the initialization process.

During collaborative discussions between ESRL and NCAR it became evident that the two different DFI implementations contained very similar components that could be combined for the benefit of all users. At this point the two groups created a single merged executable DFI system that maximized both the flexibility in the DFI runtime options along with the time series filter choices, and, in addition, eliminated the use of intermediate data output. The results of the combined efforts have since then been made available to the user community through the WRF Model releases.

3. Methodology

The RAP numerical model code used in the simulations shown here is originally based upon the WRF version 3.5.1 release. The simulations are conducted using the standard operational RAP configuration; employing a 759×568 horizontal gridpoint domain with

approximately 13.5-km grid spacing and 51 vertically stretched levels (BEN). The suite of physical parameterizations used in these simulations are from an early implementation of the RAP (BEN): the RUC land surface model (Smirnova et al. 1997, 2000), the Mellor–Yamada–Nakanishi–Niino (MYNN) boundary layer (Nakanishi and Niino 2006), the Grell–Freitas cumulus scheme (Grell and Freitas 2013), the Rapid Radiative Transfer Model for GCM (RRTMG) shortwave and longwave radiation (Iacono et al. 2008), and the Thompson microphysics (Thompson et al. 2004) parameterizations.

To examine the impact of the DFI on the RAP forecasts, a series of 1-h cycled retrospective simulations for the 7-day period from 0000 UTC 16 May to 0000 UTC 23 May 2013 were conducted with and without the DFI. In both retrospective tests, the RAP was initialized hourly and integrated to 18 h. Prior to each initialization, the GSI data assimilation package was utilized to produce a model analysis using the 1-h output forecast from the previous filtered analysis as the background (BEN). Atmospheric variables were partially cycled, wherein a “new” atmospheric state was introduced every 12 h at 0900 and 2100 UTC following a 6-h offline RAP cycling initialized from operational Global Forecast System (GFS) 3-h forecasts valid at 0300 and 1500 UTC, respectively. Within the DFI-initialized retrospective simulations, the DFI was run for a cycle period of 40 min with a 40-s time step, consisting of a 20-min backward integration (inviscid, adiabatic, and thermodynamically reversible) while applying a Dolph filter weighting over the period. Then, starting with the filtered fields valid 10 min prior to analysis time, a 20-min forward integration with full physics including the mixing/dissipation terms is integrated and all prognostic variables are subsequently filtered. The 20-min integration period stems from Eq. (6) in Lynch (1997) that estimates the minimum time span to reduce the maximum amplitudes in the stop band, which here is also frequencies greater than 1 h^{-1} , to less than 10% their original value. The forward process results in a set of filtered model fields at the analysis time (Fig. 1). The observed relative humidity and hydrometeor variables are preserved at the initialization time. The unfiltered relative humidity and filtered temperature are used in combination to calculate the initialized water vapor mixing ratios after the final filtered states are computed. Thus, a total of 168 RAP model initializations and retrospective simulations using the operational configuration (BEN) were made for both test sets during this 7-day study window.

An improvement to this methodology has been suggested in which the background states provided to the

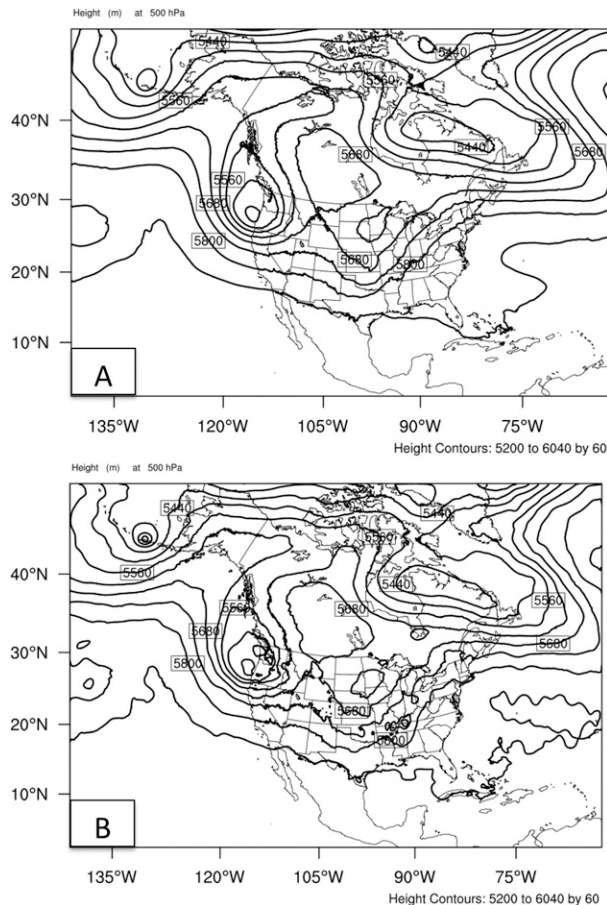


FIG. 2. The 500-hPa geopotential height (solid, m) contours at 0000 UTC 22 May 2013, as produced by the WRF Model both (a) with and (b) without the DFI.

GSI are also filtered. Then the final initialized analysis fields calculated as the sum of the background and difference between the filtered analysis and the filtered background could potentially reduce imbalances due to the analysis while maintaining the dynamically consistent small scales generated by the forecast model. This new procedure is a topic of future research and will not be addressed in this manuscript.

4. Test results

To demonstrate how the DFI reduces the overall high-frequency pressure perturbations (or IGW noise) in the model initial state, plots of 500-hPa geopotential height for the 0000 UTC 22 May 2013 initial conditions are shown in Fig. 2. In the non-DFI initialization (i.e., the GSI analysis; Fig. 2b), small-scale geopotential height perturbations are evident. The DFI clearly reduces these perturbations (Fig. 2a), especially in regions away from complex topography. As a result, the excitation of

spurious gravity waves at the outset of the model integration is significantly reduced, allowing a more realistic depiction of large-scale cloud and precipitation structures early in the simulation. This is in agreement with previous studies that reported that the DFI produces consistent cloud fields and vertical motions at initialization that were not analyzed, as well as reducing spinup issues (e.g., Chen and Huang 2006; Huang and Sundqvist 1993).

The DFI-initialized retrospective test generally exhibited reduced forecast errors compared to those in the non-DFI test. Figure 3 shows the 1-h forecast root-mean-square error (RMSE) vertical profiles of temperature, relative humidity, and horizontal wind speed, averaged over the contiguous United States (CONUS) at both 0000 and 1200 UTC, as verified against radiosonde measurements (RAOBs). Compared to the non-DFI simulations, the DFI-initialized test shows that the RMSEs are reduced for temperature by (~ 0.1 K) and wind velocity by (~ 0.25 m s^{-1}) over most of the troposphere. Although cycling in the RAP allows forecast outcomes to influence subsequent runs, Fig. 3 provides strong evidence that the DFI can improve short-term forecasts of mass and momentum fields, in addition to noise reduction (as seen in Fig. 2) at the outset of a run. This improvement is partly from the direct effect of DFI on the analysis and partly from the improvement on subsequent backgrounds (1-h forecasts) in the data assimilation.

Figure 4 shows simulated radar composite reflectivity over the eastern two-thirds of CONUS at 0000 UTC 22 May 2013 from 1-h simulations of both retrospective tests. Comparing with the observed composite reflectivity mosaic suggests that both runs are able to capture many of the observed regions of precipitation. For example, the zones of precipitation across the northern Great Plains and over New England are captured well by both simulations. In addition, both simulations depict north-south-oriented bands of convective precipitation in the southeastern United States. However, the intensity of the deep convective elements is much stronger in the simulations that were conducted without DFI, which more closely matches the radar observations. While the previous figures demonstrate the effectiveness of the DFI at reducing the initial noise, the DFI unfortunately also reduces the intensity and affects morphology of parameterized convective precipitation early on in the retrospective simulations. For example, the radar-observed convection from Texas to Tennessee (zoomed-in panel in Fig. 4c) has peak reflectivity values from 45 to 50 dBZ. The reflectivity values derived from the simulations without DFI (zoomed-in panel in Fig. 4b) are also in the 45–50-dBZ

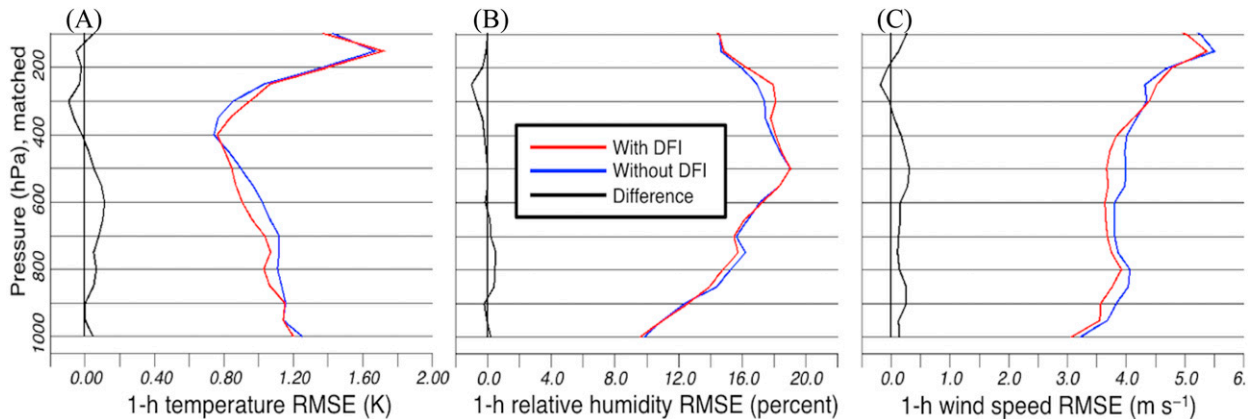


FIG. 3. Mean vertical profiles of root-mean-square error (RMSE) in RAP retrospective simulations vs RAOBs for (a) temperature, (b) relative humidity, and (c) wind speed across CONUS. The lines depict the 1-h forecast average results from the period 16–23 May 2013 for experiments using DFI (red lines) and the experiments without DFI (blue lines) period, as well as the no-DFI less the DFI experiment differences (black lines).

range with the structure and location in close approximation to the observed precipitation. In contrast, the simulations with DFI (zoomed-in panel in Fig. 4a) have peak reflectivity values in the 40–45-dBZ range with the location and computed reflectivity structure suggesting a weaker cold pool and slower propagation speed. Hence, while using the DFI has not noticeably changed the regions of simulated stratiform precipitation, the parameterized deep moist convection, which relies on simulated small-scale triggering mechanisms, can be impacted.

To further explore the impact of DFI on RAP precipitation forecasts, the 6-h critical success index (CSI) and frequency bias (Wilks 1995) for the “with DFI” (red lines) and “without DFI” (blue lines) retrospective simulations for the time period of 16–23 May 2013 are examined (Fig. 5). In these plots, higher values of CSI and frequency bias values of 1 are preferred. These scores show that the retrospective simulations that include DFI have negligibly lower forecast skill and higher-frequency bias for light precipitation amounts (i.e., 6-h accumulations < 1 in.). Also Fig. 5 exemplifies that for heavy precipitation amounts (i.e., 6-h accumulations > 1 in.), the forecast skill is better for the simulations including DFI and they are biased closer to unity compared to the simulations without DFI. These precipitation skill scores indicate that simulations with DFI have reduced heavy precipitation errors often associated with over prediction of convective rainfall rates, but this comes at the expense of increased errors for light-to-moderate precipitation.

A previously mentioned constraint of the twice DFI option is the adiabatic backward integration. The absence of diabatic processes from the backward

integration may be detrimental to mesoscale and storm-scale forecasting applications, including the precipitation processes, and could lead to critical errors in real-time forecasts (Zhu et al. 2013; Pan et al. 2014). This is due to the DFI data filtering significantly attenuating modes with frequencies higher than the filter cutoff. For the RAP, the cutoff frequency was chosen to be 1 h and so the DFI is significantly reducing the amplitude of shorter-lived mesoscale components that are potential triggers for parameterized deep moist convection, while preserving the synoptic-scale components. However, these mesoscale components may be vital to forecast accuracy during the warm season, because simulated deep moist convection could organize upscale into long-lived mesoscale convective systems that induce synoptic-scale mass and momentum adjustments. Thus, while the DFI methodology in the RAP forecast benefits the generation of short-term forecasts by removing noise from the initial fields and reducing the errors in the momentum and mass fields, it also could remove the high-frequency perturbations that aid the model parameterizations in producing the observed deep moist convection. It is for this reason that radar and lightning assimilation in the DFI (BEN; Weygandt and Benjamin 2007; Weygandt et al. 2008) remain topics of research and model development.

5. Summary and conclusions

Imbalances in the model analysis fields may be caused by data interpolation and analysis assimilation methods. A DFI capability has been implemented in the WRF Model and is presently utilized by the real-time RAP. To examine the impact of the DFI on RAP model

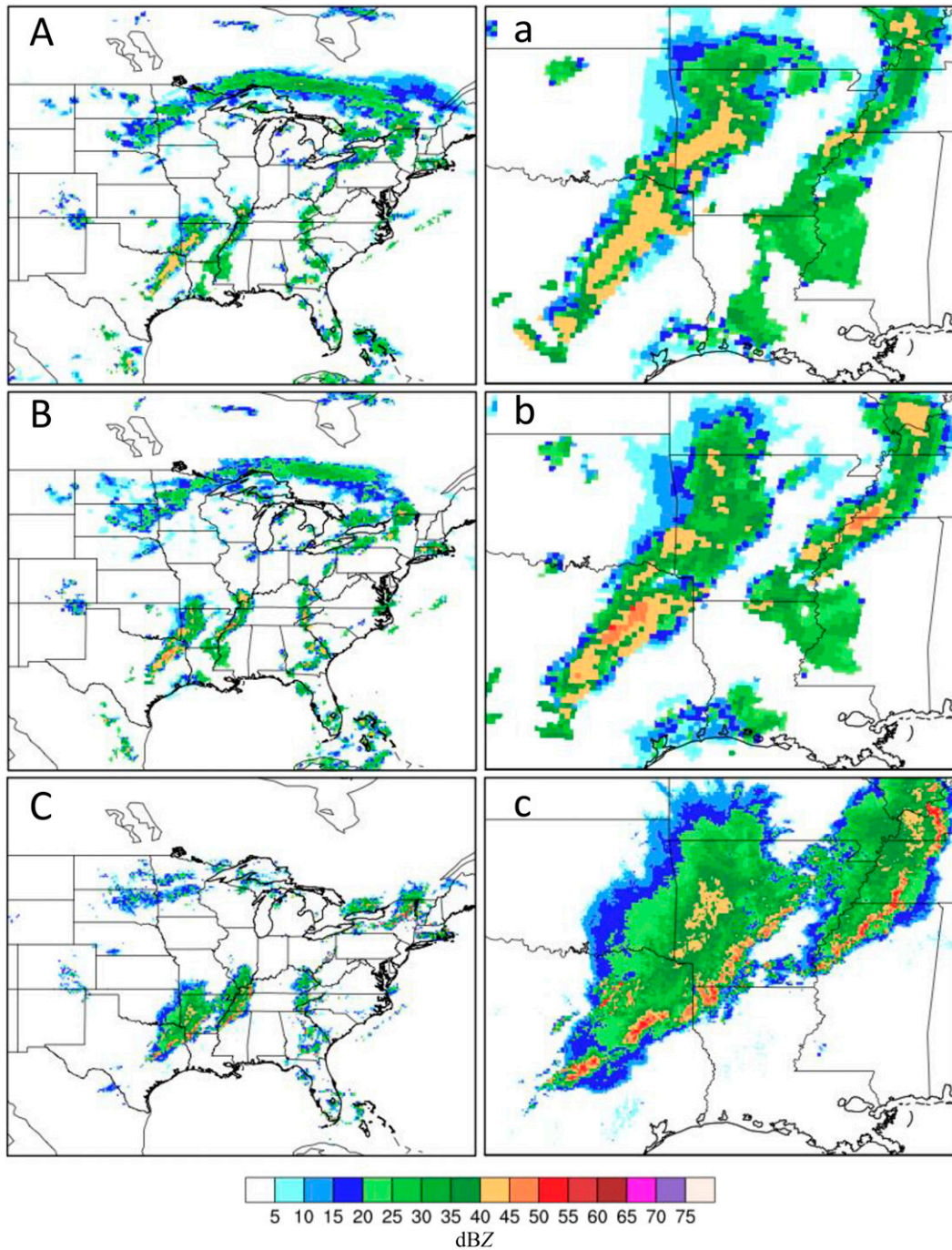


FIG. 4. Composite reflectivity for the section of CONUS domain east of 109°W longitude for a 1-h forecast ending at 0000 UTC 22 May 2013. The panels are produced from the retrospective simulations run (top) [(A) and the corresponding zoomed-in (a)] with DFI and (middle) [(B) and the corresponding zoom-in (b)] without DFI initialized at 2300 UTC 21 May 2013. The computed composite reflectivity values (dBZ) for (A) and (B) are provided by the color bar at the base of the image. (bottom) [(C) and the zoomed-in (c)] The observed composite radar for 0015 UTC 22 May 2013 is provided with the color bar providing the observed reflectivity values (dBZ).

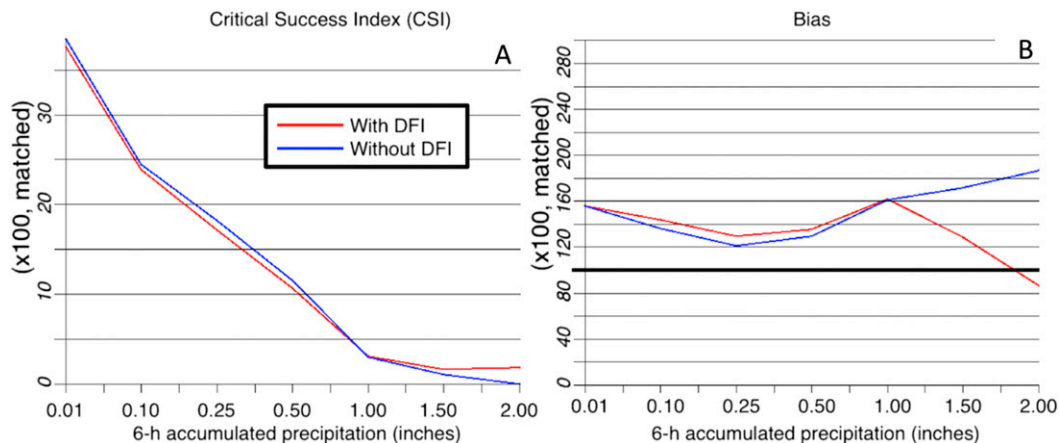


FIG. 5. (a) Critical success index (CSI) and (b) frequency bias of simulated 6-h precipitation, stratified by precipitation amount, for RAP retrospective tests performed with and without DFI (red and blue curves, respectively). CSI and frequency bias are calculated using 0–6-h forecast accumulated precipitation amounts verified against the stage-IV dataset, subject to a 40-km “neighborhood” average. CSI and frequency bias are then composited for the period of 16–23 May 2013 across the portion of the CONUS east of 100°W. For CSI, higher values are preferred, whereas a frequency bias of 100 is optimal (shown with a bold horizontal line).

performance, 7-day RAP retrospective tests, with hourly model runs to 18h were performed with DFI and non-DFI initializations. Results from the simulations suggest that the DFI has reduced numerical noise at the outset of model integration. Moreover, short-term forecast performance for some variables in our tests has been improved by the DFI. However, despite the improvements to the initial state and short-term forecast fields, there still remains a need for additional improvements to better capture deep moist convective precipitation fields. Improved procedures, such as radar reflectivity and lightning assimilation, for initializing diabatic processes central to short-range forecast models like the RAP will be discussed in a future manuscript.

Acknowledgments. The authors wish to acknowledge the contributions of Eric James and John Osborn for their review of the manuscript. We also thank the anonymous reviewers for their insightful comments that help to significantly improve this manuscript. Finally, the authors also acknowledge NCAR/MMM for their collaboration and support in developing the WRF Model.

REFERENCES

- Benjamin, S. G., and Coauthors, 2004: An hourly assimilation–forecast cycle: The RUC. *Mon. Wea. Rev.*, **132**, 495–518, doi:10.1175/1520-0493(2004)132<0495:AHACTR>2.0.CO;2.
- , and Coauthors, 2007: From the radar-enhanced RUC to the WRF-based Rapid Refresh. *22nd Conf. on Weather Analysis and Forecasting/18th Conf. on Numerical Weather Prediction*, Park City, UT, Amer. Meteor. Soc., J3.4. [Available online at https://ams.confex.com/ams/22WAF18NWP/techprogram/paper_124827.htm.]
- , and Coauthors, 2009: Technical review of Rapid Refresh/RUC project. NOAA/ESRL/GSD internal review. [Available online at http://ruc.noaa.gov/pdf/RR-RUC-TR_11_3_2009/pdf.]
- Chen, M., and X.-Y. Huang, 2006: Digital filter initialization for MM5. *Mon. Wea. Rev.*, **134**, 1222–1236, doi:10.1175/MWR3117.1.
- Grell, G. A., and S. R. Freitas, 2013: A scale and aerosol aware stochastic convective parameterization for weather and air quality modeling. *Atmos. Chem. Phys. Discuss.*, **13**, 23 845–23 893, doi:10.5194/acpd-13-23845-2013.
- Huang, X.-Y., and P. Lynch, 1993: Diabatic digital filter initialization: Application to the HIRLAM model. *Mon. Wea. Rev.*, **121**, 589–603, doi:10.1175/1520-0493(1993)121<0589:DDFIAT>2.0.CO;2.
- , and H. Sundqvist, 1993: Initialization of cloud water content and cloud cover for numerical prediction models. *Mon. Wea. Rev.*, **121**, 2719–2726, doi:10.1175/1520-0493(1993)121<2719:IOCWCA>2.0.CO;2.
- , and X. Yang, 2002: A new implementation initialization of digital filtering schemes for HIRLAM. HIRLAM Tech. Rep. 53, 36 pp.
- , M. Chen, W. Wang, J.-W. Kim, W. Skamarock, and T. Henderson, 2007: Development of Digital Filter Initialization for WRF and its implementation at IUM. Preprints, *Eighth Annual WRF User’s Workshop*, Boulder, CO, NCAR, P5.4. [Available online at http://www2.mmm.ucar.edu/wrf/users/workshops/WS2007/abstracts/p5-4_Huang.pdf.]
- Iacono, M. J., J. S. Delamere, E. J. Mlawer, M. W. Shephard, S. A. Clough, and W. D. Collins, 2008: Radiative forcing by long-lived greenhouse gases: Calculations with the AER radiative transfer models. *J. Geophys. Res.*, **113**, D13103, doi:10.1029/2008JD009944.
- Lynch, P., 1997: The Dolph–Chebyshev window: A simple optimal filter. *Mon. Wea. Rev.*, **125**, 655–660, doi:10.1175/1520-0493(1997)125<0655:TDCWAS>2.0.CO;2.

- , and X.-Y. Huang, 1992: Initialization of the HIRLAM model using a digital filter. *Mon. Wea. Rev.*, **120**, 1019–1034, doi:10.1175/1520-0493(1992)120<1019:IOTHMU>2.0.CO;2.
- , and —, 1994: Diabatic initialization using recursive filters. *Tellus*, **46A**, 583–597, doi:10.1034/j.1600-0870.1994.t014-00003.x.
- , D. Giard, and V. Ivanovici, 1997: Improving the efficiency of a digital filtering scheme. *Mon. Wea. Rev.*, **125**, 1976–1982, doi:10.1175/1520-0493(1997)125<1976:ITEOAD>2.0.CO;2.
- Nakanishi, M., and H. Niino, 2006: An Improved Mellor–Yamada level-3 model: Its numerical stability and application to a regional prediction of advection fog. *Bound.-Layer Meteor.*, **119**, 397–407, doi:10.1007/s10546-005-9030-8.
- Pan, Y., K. Zhu, M. Xue, X. Wang, M. Hu, S. G. Benjamin, S. S. Weygandt, and J. S. Whitaker, 2014: A GSI-based coupled EnSRF–En3DVar hybrid data assimilation system for the operational Rapid Refresh model: Tests at a reduced resolution. *Mon. Wea. Rev.*, **142**, 3756–3780, doi:10.1175/MWR-D-13-00242.1.
- Peckham, S. E., T. G. Smirnova, S. Benjamin, J. Brown, X.-Y. Huang, and M. Chen, 2008: Implementation and testing of WRF DFI. Preprints, *Ninth WRF Users' Workshop*, Boulder, CO, NCAR, P1.3. [Available online at http://www.researchgate.net/publication/228585676_P1_3_Implementation_and_testing_of_WRF_DFI.]
- Skamarock, W. C., and J. B. Klemp, 2008: A time-split non-hydrostatic atmospheric model for weather and forecasting applications. *J. Comput. Phys.*, **227**, 3465–3485, doi:10.1016/j.jcp.2007.01.037.
- Smirnova, T. G., J. M. Brown, and S. G. Benjamin, 1997: Performance of different soil model configurations in simulating ground surface temperature and surface fluxes. *Mon. Wea. Rev.*, **125**, 1870–1884, doi:10.1175/1520-0493(1997)125<1870:PODSMC>2.0.CO;2.
- , —, —, and D. Kim, 2000: Parameterization of cold season processes in the MAPS land-surface scheme. *J. Geophys. Res.*, **105**, 4077–4086, doi:10.1029/1999JD901047.
- , S. E. Peckham, S. G. Benjamin, and J. M. Brown, 2009: Implementation and testing of WRF Digital Filter Initialization (DFI) at NOAA/Earth System Research Laboratory. *23rd Conf. on Weather Analysis and Forecasting/19th Conf. on Numerical Weather Prediction*, Omaha, NE, Amer. Meteor. Soc., 18A.4. [Available online at https://ams.confex.com/ams/23WAF19NWP/techprogram/paper_154325.htm.]
- Thompson, G., R. M. Rasmussen, and K. Manning, 2004: Explicit forecasts of winter precipitation using an improved bulk microphysics scheme. Part I: Description and sensitivity analysis. *Mon. Wea. Rev.*, **132**, 519–542, doi:10.1175/1520-0493(2004)132<0519:EFOWPU>2.0.CO;2.
- Weygandt, S. S., and S. Benjamin, 2007: Radar reflectivity-based initialization of precipitation systems using a diabatic digital filter within the Rapid Update Cycle. *22nd Conf. on Weather Analysis and Forecasting/18th Conf. on Numerical Weather Prediction*, Park City, UT, Amer. Meteor. Soc., 1B.7. [Available online at https://ams.confex.com/ams/22WAF18NWP/techprogram/paper_124540.htm.]
- , S. G. Benjamin, T. G. Smirnova, and J. M. Brown, 2008: Assimilation of radar reflectivity data using a diabatic digital filter within the Rapid Update Cycle. *12th Conf. on Integrated Observing and Assimilation Systems for Atmosphere, Oceans, and Land Surface*, New Orleans, LA, Amer. Meteor. Soc., 8.4. [Available online at https://ams.confex.com/ams/88Annual/techprogram/paper_134081.htm.]
- Wilks, D. S., 1995: *Statistical Methods in the Atmospheric Sciences: An Introduction*. Elsevier, 467 pp.
- Zhu, K., Y. Pan, M. Xue, X. Wang, J. S. Whitaker, S. G. Benjamin, S. S. Weygandt, and M. Hu, 2013: A regional GSI-based ensemble Kalman filter data assimilation system for the rapid refresh configuration: Testing at reduced resolution. *Mon. Wea. Rev.*, **141**, 4118–4139, doi:10.1175/MWR-D-13-00039.1.